ACS OMEGA

http://pubs.acs.org/journal/acsodf

Article

# Triglyceride Conversion of Waste Frying Oil up to 98.46% Using Low Concentration $K^+$/CaO Catalysts Derived from Eggshells

Mosharof Hossain,* Nuzhat Muntaha, Lipiar Khan Mohammad Osman Goni, Mohammad Shah Jamal, Mohammad Abdul Gafur, Dipa Islam, and Abu Naieum Muhammad Fakhruddin

Cite This: *ACS Omega* 2021, 6, 35679–35691

Read Online

ACCESS | Metrics & More | Article Recommendations | Supporting Information

**ABSTRACT:** In this study, biodiesel, also known as fatty acid methyl ester (FAME), was synthesized from multi-stage frying waste soybean oil using chicken eggshell-derived CaO and potassium-impregnated $K^+$-CaO heterogeneous catalysts. Potassium-impregnated catalysts (1.25% $K^+$-CaO, 2.5% $K^+$-CaO, and 5% $K^+$-CaO) were developed by treating the calcined waste eggshell powder with KOH in different wt % ratios. The catalysts were characterized using FTIR, XRD, FESEM, EDS, BET, and particle size analysis techniques. Box–Behnken design-based optimization was exploited to optimize the reaction parameters. A maximum yield of 98.46%, calculated via $^1$H NMR, was achieved following a 5% $K^+$ doping, 12:1 methanol to oil molar ratio, 3% catalyst amount, 180 min reaction time, and 65 °C reaction temperature. The catalyst (5% $K^+$-CaO) responsible for maximum biodiesel production was found to be highly reusable, with a 30.42% conversion decrease in activity after eight cycles of reuse. Gas chromatography was used to determine the composition of FAME produced from different cycles of waste soybean oil. Physicochemical parameters of the synthesized biodiesel were found to be compatible with EN and ASTM standards. This study has shown that the waste eggshell-derived heterogeneous catalysts have significant catalytic activity at relatively low $K^+$ doping and catalyst loading leading to high biodiesel conversion.

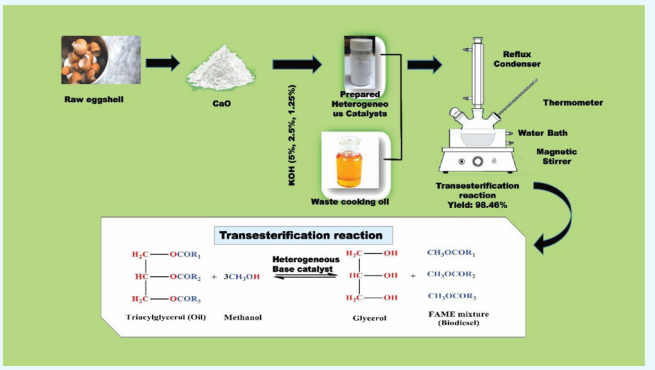


## 1. INTRODUCTION

Nearly 81.7% of the world's energy demand is met by fossil fuels according to the International Energy Agency (IEA).[1] Mitigation of non-renewable energy sources like natural gases, coal, and petroleum and their negative impact on the environment have prompted humankind to look for alternative energy sources. Renewable energy sources can play an important role in dealing with the global energy crisis. As economically viable and ecologically sustainable alternative energy sources to conventional petrodiesel, liquid biofuels have caught the attention of researchers.[2] Fatty acid alkyl esters, generally known as biodiesel, derived from organic sources, such as vegetable oils, animal fat, or waste cooking oil, are a proven alternative to conventional diesel owing to its significant and non-toxic fuel properties.[3] Single-step transesterification and two-step esterification and transesterification are the popular traditional chemical reaction processes for biodiesel production. The transesterification reaction can occur using an acid/base catalyst in the presence of methanol/ethanol if the triglyceride feedstock contains less than 2% of free fatty acid (FFA).[4,5] Due to food scarcity, the use of edible oils as feedstocks for biodiesel production can be a concerning matter. As a consequence, researchers are looking forward to non-edible oils like rubber seed, Jatropha seed, and Karanja seed oil for their use as potential feedstocks for biodiesel production.[2,6−8] However, owing to the scarcity of non-edible oils and the consequential high cost of biodiesel produced from them, waste cooking oil (WCO) has become a reliable source for biodiesel production.[9] Choice of feedstock mainly contributes to the final product's price, and, as WCO is widely available across the globe, producing biodiesel from it is an economically very viable option.

Usually, homogeneous catalysts, such as NaOH and KOH, have been used for transesterification on a marketable scale for biodiesel production. They facilitate higher reaction rates in lower reaction temperature and other mild conditions.[10] However, homogeneous catalysts are expensive, corrosive to the reactors, responsible for secondary pollution, and inconvenient to reuse. These catalysts, understandably, generate

Received: October 7, 2021
Accepted: December 3, 2021
Published: December 15, 2021

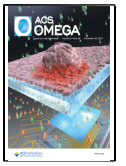

complications in the separation and purification steps of biodiesel production. In contrast, heterogeneous catalysts are more effective, non-corrosive, economical, eco-friendly, and reusable.[11] Therefore, heterogeneous catalysts are being preferred than homogeneous ones for the transesterification reaction process. To this date, several heterogeneous catalysts have been developed; such as sugar factory sludge,[12] lipase immobilized biochar,[7] solid aluminum hydrogen sulfate,[13] sodium hydroxide modified anthill,[14] etc.

Due to higher stability and attractive catalytic activity, waste eggshell (WES) and chicken bone-derived CaO-based catalysts are suitable for the transesterification process. Due to the high abundance of WES and $CaCO_3$ associated with them, they are being explored heavily as a viable and economical source of the heterogeneous catalyst.[15,16] In the present study, WES, therefore, has been selected for heterogeneous catalyst synthesis. CaO being the fundamental constituent of calcined eggshells has low catalytic activity and high moisture sensitivity. Impregnation of metal oxide in calcium oxide is an appropriate pathway to overcome these drawbacks.[10] For impregnation, potassium hydroxide aqueous solution was chosen in this study because potassium oxide can work as an excellent basic oxide. The traditional one factor at a time optimization process makes the whole transesterification process time consuming and resource intensive.[17] In this study, the Box Behnken design (BBD)-based response surface methodology (RSM) has been exploited for optimizing chemical processes with a view of finding the economically most viable route to the maximum biodiesel yield.

This study focused on the development of a heterogeneous base catalyst CaO from inexpensive biomass source WES and impregnation with KOH to produce biodiesel from waste soybean oil (WSO). There are numerous reports on the derivation of CaO from WES and impregnation with Na[6], Zn[10], and Cu/Zn[18] for biodiesel production. There are also reports about producing biodiesel by commercially available CaO.[19,20] Furthermore, some works of WES-derived CaO being impregnated by KOH have also been reported earlier.[20,21] However, our work demonstrates WES-derived CaO being impregnated with KOH at very low (1.25%, 2.5%, 5% w/w) concentrations and with the minimum amount of catalyst loading for producing biodiesel from multi-stage frying soybean oil. The catalyst was reused efficiently until the eighth cycle, which shows its high catalytic activity. To this date, other publications about converting WCO to biodiesel rarely discussed about frying cycles, time, and temperature of the used WCO. The present study provides primary data for the frying cycle of the raw material (soybean oil), frying time, and temperature of frying WSO, which, to the best of our knowledge, has not been reported yet. The WSO was collected after every 4th frying cycle until 16th cycle for biodiesel production. Four parameters, namely, doping of potassium, catalyst concentration, reaction time, and methanol to oil ratio, were investigated to optimize the transesterification process to achieve the maximum biodiesel yield.

## 2. RESULTS AND DISCUSSION

**2.1. Characterization of Catalyst.** *2.1.1. Fourier Transforms Infrared Spectroscopy (FT-IR) Analysis.* The FT-IR spectra of catalysts (CaO and $K^+$-doped CaO) are displayed in Figure 1. The band around 3645 $cm^{-1}$ could be attributed to the $OH^-$ stretching vibration of the hydroxy-functional groups attached to CaO.[22] At 1431 $cm^{-1}$, the IR signal was comparatively weak and can be correlated to the stretching

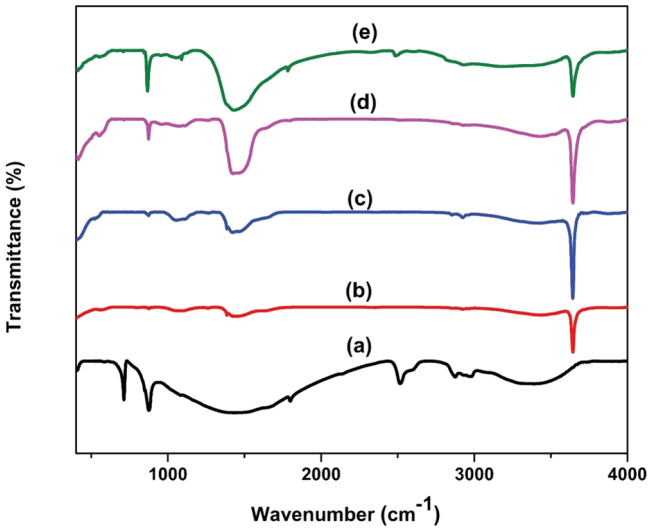


**Figure 1.** FTIR spectra of (a) RES, (b) CaO, (c) 1.25% $K^+$-CaO, (d) 2.5% $K^+$-CaO, and (e) 5% $K^+$-CaO.

vibrations of the $CO_3^{2-}$ group in various structural sites. The spectra show bands at 1061 and 866 $cm^{-1}$, matching mono and bidentate carbonates' vibration modes, respectively.[23] The strong band at 412 $cm^{-1}$ can be attributed to the vibrations of the Ca−O bond.[24,25]

*2.1.2. X-ray Diffraction (XRD) Analysis.* Figure S1 and Figure 2 show the XRD patterns of RES, CaO, and $K^+$-doped catalysts.

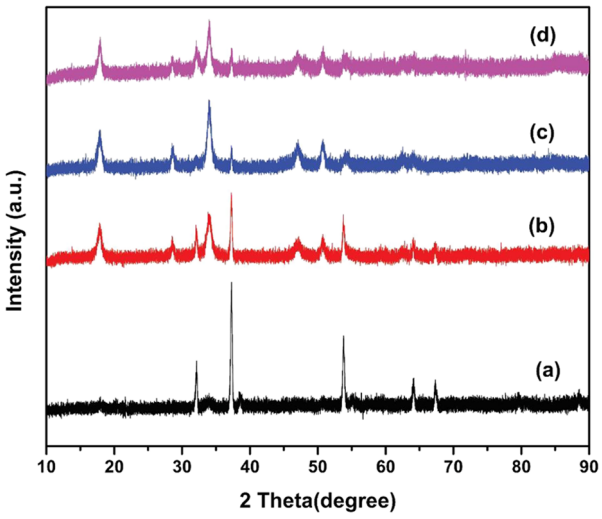


**Figure 2.** XRD patterns of (a) CaO, (b) 1.25% $K^+$-CaO, (c) 2.5% $K^+$-CaO, and (d) 5% $K^+$-CaO calcined at 900 °C.

The appearance of sharp peaks at different 2$\theta$ values hints at the presence of crystalline planes. Peaks at 2$\theta$ values of 32.14, 37.30, 53.82, 64.18, and 67.34° can be indexed to (111), (200), (220), (311), and (222) planes, respectively, of cubic CaO (JCPDS file no. 481467), as confirmed by the study of Rahman et al.[18] However, as the $K^+$ loading increases from 1.25 to 5%, the most prominent peak at 37.30° decreases in intensity, suggesting the distortion of the CaO lattice by the impregnation of $K^+$. The same trend has been noticed for the peaks at 53.82, 64.18, and 67.34° as well.

The average crystallite size of the maximum intensity peak corresponding to the (200) plane was determined using the


https://doi.org/10.1021/acsomega.1c05582
ACS Omega 2021, 6, 35679−35691

Debye−Scherrer equation, eq 1,[26] where $D$, $\lambda$, $\beta$, and $\theta$ represent the average crystallite size, X-ray wavelength, full width at half-maximum of the chosen peak, and Bragg's angle, respectively. The successive decrease of the average crystallite size corresponding to the peak at 37.30° of undoped and doped CaO samples is represented in Table 1.

$$D = \frac{0.9\lambda}{\beta \cos \theta} \quad (1)$$

**Table 1. $K^+$ Loaded in CaO and Crystalline Size Variation**

| $K^+$ concentration (%) | crystallite size (nm) |
|---|---|
| 0.00 | 27.11 |
| 1.25 | 23.23 |
| 2.50 | 16.39 |
| 5.00 | 11.68 |

*2.1.3. Field Emission Scanning Electron Microscopy (FESEM) Analysis.* The surface morphologies of RES and the prepared catalysts (CaO, 1.25% $K^+$-CaO, 2.5% $K^+$-CaO, and 5% $K^+$-CaO) investigated by FESEM are presented in Figure S2 and Figure 3a−d. The surface of undoped CaO shows the presence of uniform-sized, spherical-shaped particles in a regular matrix. However, as the amount of $K^+$ doping (1.25%, 2.5%, and 5% w/w) increases, additional rod- and dumbbell-shaped particles with irregular size appear in a nonuniform manner, covering almost the entire surface of the prepared catalysts. Those spherical-shaped particles were mainly the contribution of active $K^+$ species. On the other hand, the irregularities observed in the doped catalysts may have been contributed by forming clusters of $K^+$-CaO particles while they were prepared and calcined.

*2.1.4. Energy Dispersive X-ray Spectroscopy (EDS) Analysis.* The EDS spectra of RES, CaO, 1.25% $K^+$-CaO, 2.5% $K^+$-CaO, and 5% $K^+$-CaO catalysts are shown in Figure S3 and Figure 4. EDS spectra of doped catalyst samples show the presence of Ca, O, and K, whereas that of the undoped sample indicates the presence of Ca and O only. A maximum of 12.51% (by atom) K was found for 5% $K^+$-CaO.

*2.1.5. BET Analysis.* Different surface characteristics, such as surface area, pore volume, and pore diameter of CaO and 5% $K^+$-CaO catalysts determined via BET analysis, are presented in Table 2. The surface area of CaO and 5% $K^+$-CaO were determined to be 5.69 and 12.14 $m^2/g$, respectively. On the

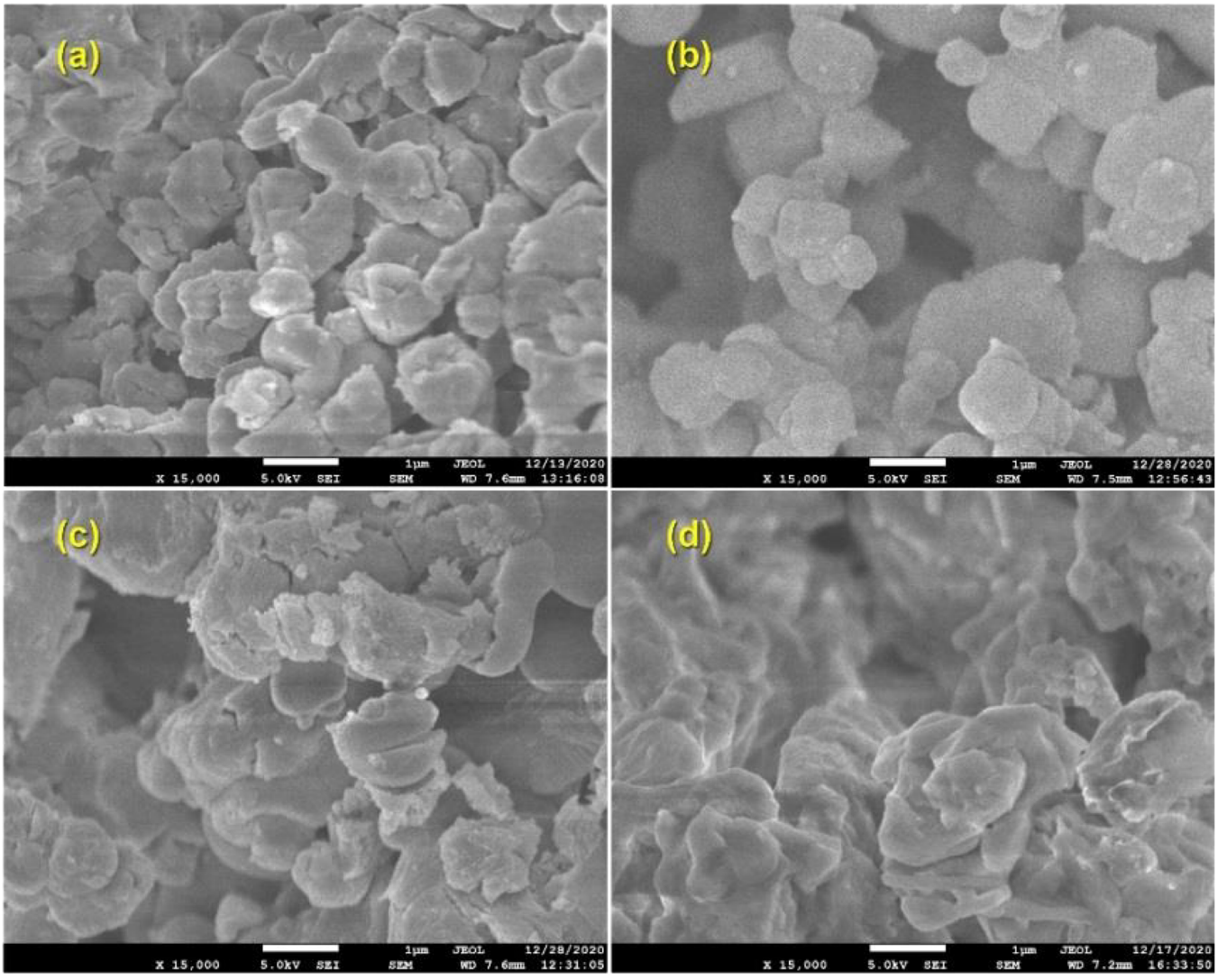


**Figure 3.** FESEM images (scale bar: 1 $\mu$m) of (a) CaO, (b) 1.25% $K^+$-CaO, (c) 2.5% $K^+$-CaO, and (d) 5% $K^+$-CaO calcined at 900 °C.



https://doi.org/10.1021/acsomega.1c05582
ACS Omega 2021, 6, 35679−35691

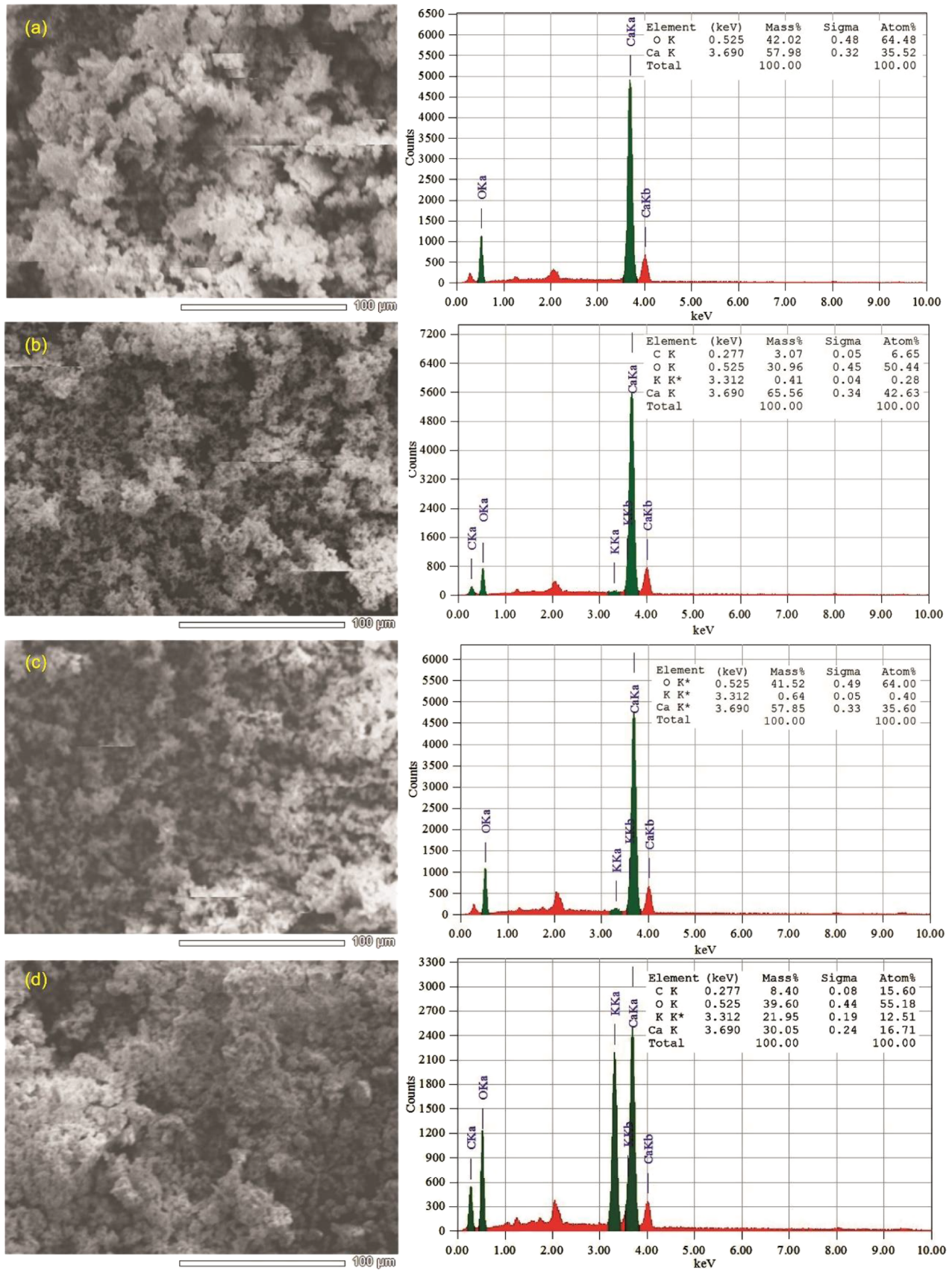


**Figure 4.** EDS spectra (right) and corresponding FESEM images (left; scale bar: 100 $\mu$m) of (a) CaO, (b) 1.25% $K^+$-CaO, (c) 2.5% $K^+$-CaO, and (d) 5% $K^+$-CaO calcined at 900 °C.



https://doi.org/10.1021/acsomega.1c05582
*ACS Omega* 2021, 6, 35679−35691

**Table 2. Surface Area, Pore Volume, and Pore Diameter of CaO and 5% $K^+$-CaO Calcined at 900 °C**

| Sl. no. | catalyst | cal. temp. (°C) | surface area ($m^2$/g) | pore volume ($cm^3$/g) | pore diameter (nm) |
|---|---|---|---|---|---|
| 1 | CaO | 900 | 5.69 | 0.0051 | 9.61 |
| 2 | 5% $K^+$-CaO | 900 | 12.14 | 0.0159 | 11.16 |

other hand, the pore volume of CaO and 5% $K^+$-CaO were found to be 0.0051 and 0.0159 $cm^3$/g. Additionally, the pore diameter of 5% $K^+$-CaO was determined to be greater than that of CaO as well. This increase in surface characteristics of the 5% $K^+$-CaO from those of CaO can be attributed to the elimination and removal of volatile matters and minerals from the WES following calcination at a very high temperature of 900 °C. However, an increased surface area of 5% $K^+$-CaO indicates that the metal-doped catalyst should have greater activity than that of undoped CaO.[27]

*2.1.6. Particle Size Analysis.* Figure 5 shows the particle size distribution of CaO and 5% $K^+$-CaO. Both distributions appear

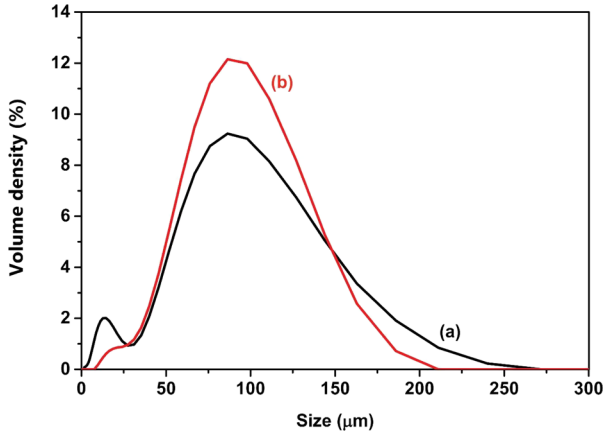


**Figure 5.** Particle size distribution of (a) undoped CaO and (b) 5% $K^+$-CaO.

to be bimodal and asymmetric, which may have been caused by the breakup of large particles during ultrasonic dispersion in deionized water. The Dv (50) values, or the median diameters, of CaO and 5% $K^+$-CaO were found to be 79.8 and 87.8 $\mu$m, respectively. The Dv (90) values for CaO and 5% $K^+$-CaO were determined to be 149 and 141 $\mu$m, respectively, meaning that 90% of the particles from both of these samples have a diameter below their corresponding Dv (90) values. D [3, 2] values , or Sauter mean diameters, which reflect the mean diameter of the fine particulates present in the sample, were found to be 34.2 and 68.1 $\mu$m for CaO and 5% $K^+$-CaO, respectively. On the other hand, D [4, 3] values, or De Brouckere mean diameters, which highlight the mean diameter of the coarse particles present in the sample, were 81.8 and 90.0 $\mu$m, respectively, for CaO and 5% $K^+$-CaO. An increase in the above-mentioned parameters of 5% $K^+$-CaO from those of CaO is indicative of the successful impregnation and agrees with the surface characteristics observed for BET analysis.

**2.2. Properties of Fried Oil.** Physical properties of both fresh and WSO are shown in Table 10. Initially, the FFA content and viscosity of the fresh soybean oil were determined to be 0.09% and 33.53 cSt, respectively. However, the FFA content and viscosity were found to increase and decrease, respectively, after the frying was completed for each cycle. As the oil keeps degrading at an elevated temperature, it was expected to produce low molecular weight compounds with low carbon numbers. Additionally, the solid content increased gradually with an increase in the frying time.

**2.3. Response Surface Methodology Analysis.** *2.3.1. Box–Behnken Design Experiments.* The experimental design consisting of 28 experiments predicted by the statistical software is shown in Table 3. The linear model was found to be the statistically most significant model, as the experimental data from all 28 experiments were found to be best fitted to a linear model. The relevant parameters associated with the model are presented in Table 4.

*2.3.2. Regression Analysis and Analysis of Variance.* The closer the value of $R^2$ (coefficient of determination) to 1, the stronger is the model.[16] An $R^2$ value of 0.9988, or 99.88%, indicates that the model can explain the variability of the response up to 99.88%. The adjusted $R^2$ value (0.9975) and predicted $R^2$ (0.9947) are pretty much near each other, indicating the fitted model's adequacy and a successful correlation between the predicted and actual response. A small value (0.389194) of the standard error of the regression (S) hints at the observed values in the experimental vs predicted yield plot, Figure 6g, being extremely close to the fitted line, confirming a good agreement between the predicted and actual response again. Table 5 shows the ANOVA for the suggested linear model. A smaller *P*-value highlights a high significance of the regression coefficients.[28] A high *F*-value of 781.17 indicates that the model is highly significant, and the associated P-value of 0.000 confirms that there is no chance of this high *F*-value occurring due to noise.[16] Owing to the *P*-values of process variables, i.e. A, B, C, and D and as well as model terms $A,^2$ $B^2$, $C^2$, $D^2$, AB, AC, AD, BC, BD, and CD being less than 0.05, or being 0.000 except that of the term CD, precisely, they are of high statistical significance. Moreover, along with statistically significant *P*- and *F*-values, a close-to-unity $R^2$ value of 0.9988 and non-significant lack-of-fit *P*-value (0.586) denote that the model is fit for prediction purpose. The mathematical relationship between the dependent (FAME yield) and three independent parameters, or to put it another way, the regression equation eq 2 for FAME yield (%) achieved via regression analysis in coded terms, is given below:

$$\begin{aligned}\text{biodiesel conversion}(\%) &= 64.10 - 2.247A - 18.311B + 5.314C + 0.3605D \\ &\quad - 1.2952A^2 + 0.6342B^2 - 0.2470C^2 - 0.002110D^2 \\ &\quad + 0.2785AB + 0.4340AC + 0.03877AD - 0.1608BC \\ &\quad + 0.06750BD + 0.00319CD \end{aligned} \quad (2)$$

*2.3.3. Effect of Process Variables on Conversion Efficiency.* The three-dimensional (3D) response surface plots (RSP) highlighting the interactions between independent reaction parameters are shown in Figure 6a–g. The interaction between $K^+$-doping and the catalyst amount is shown in Figure 6a. It is quite evident from the plot that the increase in both $K^+$-doping, except for the maximum $K^+$-doping of 5%, and catalyst amount influences the response, i.e., FAME yield, positively, which could be attributed to the increasing presence of catalysts' active sites doped with $K^+$ to facilitate the execution of the trans-esterification reaction. Figure 6b depicts the interaction between doping of $K^+$ and the methanol to oil ratio. The conversion of biodiesel increases with the increasing methanol amount in the


https://doi.org/10.1021/acsomega.1c05582
ACS Omega 2021, 6, 35679−35691

Table 3. BBD-Based Matrix for 28 Experiments Carried out by Varying Reaction Parameters

| no. of exp | A: $K^+$ doping (%) | B: catalyst loading (%) | C: methanol:oil (mol) | D: time (min) | experimental FAME yield (%) | predicted FAME yield (%) |
|---|---|---|---|---|---|---|
| 1 | 2.50 | 7 | 9 | 180 | 89.59 | 89.80 |
| 2 | 5.00 | 5 | 12 | 240 | 98.28 | 98.04 |
| 3 | 2.50 | 3 | 15 | 180 | 95.62 | 95.46 |
| 4 | 2.50 | 3 | 9 | 180 | 92.40 | 92.08 |
| 5 | 2.50 | 7 | 12 | 240 | 96.96 | 96.71 |
| 6 | 2.50 | 5 | 15 | 120 | 77.11 | 77.26 |
| 7 | 2.50 | 7 | 15 | 180 | 88.95 | 89.32 |
| 8 | 2.50 | 5 | 12 | 180 | 91.68 | 91.35 |
| 9 | 1.25 | 5 | 15 | 180 | 80.66 | 80.13 |
| 10 | 2.50 | 5 | 12 | 180 | 91.01 | 91.35 |
| 11 | 5.00 | 7 | 12 | 180 | 97.15 | 97.22 |
| 12 | 1.25 | 5 | 12 | 120 | 73.73 | 74.15 |
| 13 | 1.25 | 3 | 12 | 180 | 88.29 | 88.60 |
| 14 | 5.00 | 3 | 12 | 180 | 98.46 | 98.65 |
| 15 | 1.25 | 5 | 9 | 180 | 82.14 | 81.94 |
| 16 | 1.25 | 7 | 12 | 180 | 82.92 | 82.99 |
| 17 | 2.50 | 5 | 12 | 180 | 91.72 | 91.35 |
| 18 | 5.00 | 5 | 9 | 180 | 89.15 | 89.20 |
| 19 | 2.50 | 3 | 12 | 120 | 92.23 | 92.07 |
| 20 | 1.25 | 5 | 12 | 240 | 77.28 | 77.18 |
| 21 | 2.50 | 7 | 12 | 120 | 72.17 | 71.66 |
| 22 | 2.50 | 3 | 12 | 240 | 84.62 | 84.73 |
| 23 | 2.50 | 5 | 9 | 120 | 76.91 | 76.96 |
| 24 | 5.00 | 5 | 12 | 120 | 77.54 | 77.56 |
| 25 | 2.50 | 5 | 9 | 240 | 84.49 | 84.66 |
| 26 | 2.50 | 5 | 15 | 240 | 86.99 | 87.26 |
| 27 | 2.50 | 5 | 12 | 180 | 91.02 | 91.35 |
| 28 | 5.00 | 5 | 15 | 180 | 97.27 | 97.15 |

Table 4. Model Summary of the Best-Fitted Linear Model

| standard error of regression (S) | coefficient of determination ($R^2$) | adjusted $R^2$ | predicted $R^2$ |
|---|---|---|---|
| 0.389194 | 99.88% | 99.75% | 99.47% |

reaction mixture. This is understandable because of the increased presence of the methanol amount leading to the reactants in the transesterification reaction mixing well.[29] On the contrary, the FAME yield keeps increasing with increasing $K^+$-doping initially but decreases eventually while $K^+$-doping is maximum. This observation agrees with the XRD finding that excess $K^+$ causes distortion in the crystalline sites of CaO to make the catalyst perform poor for high $K^+$ doping.

Figure 6c represents the interaction between $K^+$-doping and reaction time. As previously observed already, the increase in $K^+$-doping makes the biodiesel conversion still follow the same trend. On the other hand, the increase in reaction time increases the biodiesel conversion sharply, owing to the reactants in the transesterification reaction getting enough time to deliver the best yields. Figure 6d highlights the interaction between the methanol to oil ratio and catalyst amount. With the increase in catalyst concentration, the yield usually decreases. It has been reported that the catalyst amount beyond the optimum will make the reaction mixture too viscous to mix well.[30] Likewise, an increase in the methanol to oil ratio seems to be causing the yield to increase. However, excess methanol, as evident from Figure 6d, can cause the polarity of the reaction medium to increase, which in turn can push glycerol into the ester phase and reduce the yield of the reaction by moving the equilibrium toward the backward direction.[31] Additionally, excess methanol can flood the reaction sites to reduce the yield.[32]

The interaction between catalyst amount and reaction time is shown in Figure 6e. Both these parameters seem to be having strong opposing trends, as the yield decreases and increases sharply with the increasing catalyst amount and reaction time, respectively. A close look at Table 3 reveals that almost all the reactions that had yields of more than 90% were allowed to go on for at least 180 min. Even though some reactions yielded more than or around 90% for the highest catalyst concentration of 7%, contradicting the trend visible in Figure 6e, it was largely due to the increased methanol to oil ratio and reaction time. Figure 6f shows the interaction between the methanol to oil ratio and reaction time. Again, the reaction time seems to be having a significant impact on biodiesel conversion, as its increase makes the biodiesel yield go up sharply. The methanol to oil ratio seems to be helping the yield increase until an optimum point beyond which its increase affects the yield negatively for reasons mentioned earlier.

*2.3.4. Optimum Reaction Conditions.* The highest yield of 98.46% (exp 14) was achieved for 5% $K^+$-doping, 3% catalyst amount, 12:1 methanol to oil ratio, and 180 min reaction time. Interestingly, another high yield of 98.28% (exp 2) was achieved for 5% catalyst loading and 240 min reaction time, while other parameters are the same as that of exp 14. However, since an increased catalyst loading and reaction time can add to the cost behind the production of biodiesel industrially, the experimental conditions of exp 14 can be considered as optimum reaction conditions.

**2.4. $^1$H NMR Analysis for Biodiesel Conversion.** Biodiesel conversion was confirmed by $^1$H NMR spectroscopy analysis. Figure 7 shows the $^1$H NMR spectrum of FAME from exp 14. The presence of distinguishing peaks at 3.62 ppm for


https://doi.org/10.1021/acsomega.1c05582
ACS Omega 2021, 6, 35679−35691

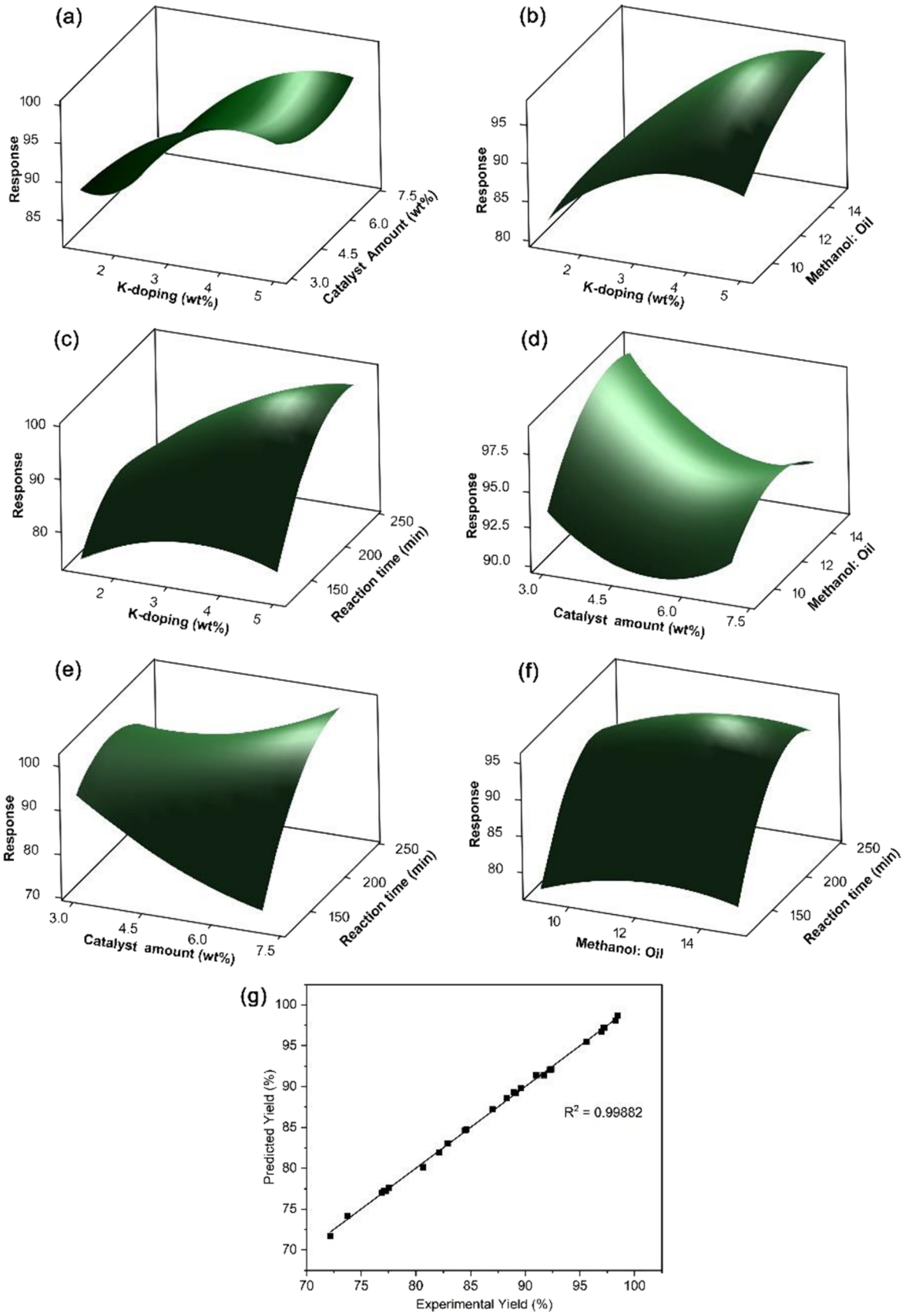


**Figure 6.** Response surface plots for the interaction of (a) $K^+$ doping and catalyst concentration, (b) $K^+$ doping and methanol to oil molar ratio, (c) $K^+$ doping and reaction time, (d) catalyst concentration and methanol to oil molar ratio, (e) catalyst concentration and reaction time, (f) methanol to oil molar ratio and reaction time, and (g) linear regression plot for experimental yield vs predicted yield.



https://doi.org/10.1021/acsomega.1c05582
*ACS Omega* 2021, 6, 35679−35691

**Table 5. ANOVA for the Suggested Linear Model**

| source | degrees of freedom | adjusted sum of squares | adjusted mean square | *F*-value | *P*-value |
|---|---|---|---|---|---|
| model | 14 | 1656.55 | 118.325 | 781.17 | 0.000 |
| linear | 4 | 864.10 | 216.024 | 1426.17 | 0.000 |
| A | 1 | 442.02 | 442.017 | 2918.15 | 0.000 |
| B | 1 | 32.59 | 32.589 | 215.15 | 0.000 |
| C | 1 | 24.88 | 24.875 | 164.22 | 0.000 |
| D | 1 | 364.61 | 364.613 | 2407.14 | 0.000 |
| square | 4 | 533.54 | 133.386 | 880.60 | 0.000 |
| $A^2$ | 1 | 93.13 | 93.127 | 614.81 | 0.000 |
| $B^2$ | 1 | 38.61 | 38.608 | 254.89 | 0.000 |
| $C^2$ | 1 | 29.66 | 29.659 | 195.81 | 0.000 |
| $D^2$ | 1 | 346.07 | 346.066 | 2284.69 | 0.000 |
| 2-way interaction | 6 | 379.51 | 63.252 | 417.58 | 0.000 |
| AB | 1 | 4.69 | 4.685 | 30.93 | 0.000 |
| AC | 1 | 25.61 | 25.607 | 169.06 | 0.000 |
| AD | 1 | 81.73 | 81.732 | 539.59 | 0.000 |
| BC | 1 | 3.72 | 3.725 | 24.59 | 0.000 |
| BD | 1 | 262.44 | 262.440 | 1732.60 | 0.000 |
| CD | 1 | 1.32 | 1.322 | 8.73 | 0.011 |
| error | 13 | 1.97 | 0.151 | | |
| lack-of-fit | 10 | 1.50 | 0.150 | 0.96 | 0.586 |
| pure error | 3 | 0.47 | 0.157 | | |
| total | 27 | 1658.52 | | | |

methoxy protons confirms the formation of FAME. On the other hand, a peak at 2.26 ppm appears for $\alpha$-$CH_2$ protons. Non-appearance of glycerine peaks in the range of 4.00−4.20 ppm further confirms the production of FAME.[33−35] For reaction 14, a maximum of 98.48% biodiesel conversion was calculated following eq 3.$^1$H NMR spectra of FAME from some additional high yield experiments are included in Figures S4−S12.

**2.5. Performance Analysis of Synthesized Catalysts.** Performances of the prepared catalysts (CaO, 1.25 wt % $K^+$-CaO, 2.5 wt % $K^+$-CaO, and 5 wt % $K^+$-CaO) were compared to some other recently reported catalysts and arediscussed in Table 6. Most of the studies reported in Table 6 are based on CaO derived from chicken eggshells. However, the studies of Farooq et al.[40] and Sirisomboonchai et al[41] were based on CaO derived from chicken bones and scallop shells, leading to 89.3% and 86.0% yield, respectively. Though Liao et al.'s[11] work on Jatropha oil using KOH doping led to 97.0% of biodiesel yield, it was achieved at the expense of high $K^+$ doping (20 wt %). On the other hand, Borah et al.'s[16] work on biodiesel production from WCO using Zn-doped CaO had a high yield of 96.74%, with a high methanol to oil molar ratio of 20:1 that can prove to be costly in an industrial setup. Oko et al.[20] worked with WCO using eggshell-derived CaO, with 7% $K^+$ doping, resulting in a low yield of 87.17% biodiesel. In this study, when CaO was used without any doping, the yield was about 88.1% with reaction variables of 3 wt % of catalyst, a reaction time of about 180 min, and a methanol to oil ratio of 12:1. At very low $K^+$ doping (1.25% with 3 wt % catalysts), the biodiesel's yield increased to 88.94%. By increasing the amount of $K^+$ doping and catalyst concentration to 2.5 and 7 wt %, respectively, a high yield of 96.96% was obtained. The best result with a very high yield of 98.46% was achieved by using 5% $K^+$ doping and the catalyst amount as low as 3 wt %. Thus, the prepared catalysts have remarkable effectiveness in delivering a high yield of biodiesel with the catalyst concentration ranging from 3−7% and a 12:1 methanol to oil ratio.

**2.6. Biodiesel Yield in a Different Frying Cycle.** The biodiesel yield, using optimum reaction conditions, from the 4th, 8th, 12th, and 16th frying cycles is shown in Table 7. The biodiesel yield from the feedstock of these frying cycles did not vary significantly. This demonstrates that the prepared catalyst's catalytic activity was not affected at all by a slight variation in physicochemical parameters of the feedstock from different frying cycles.

**2.7. FAME Composition of Soybean Oil Biodiesel in Different Cycles.** The FAME composition of multi-cycle WSO biodiesel determined by GC is given in Table 8. No significant

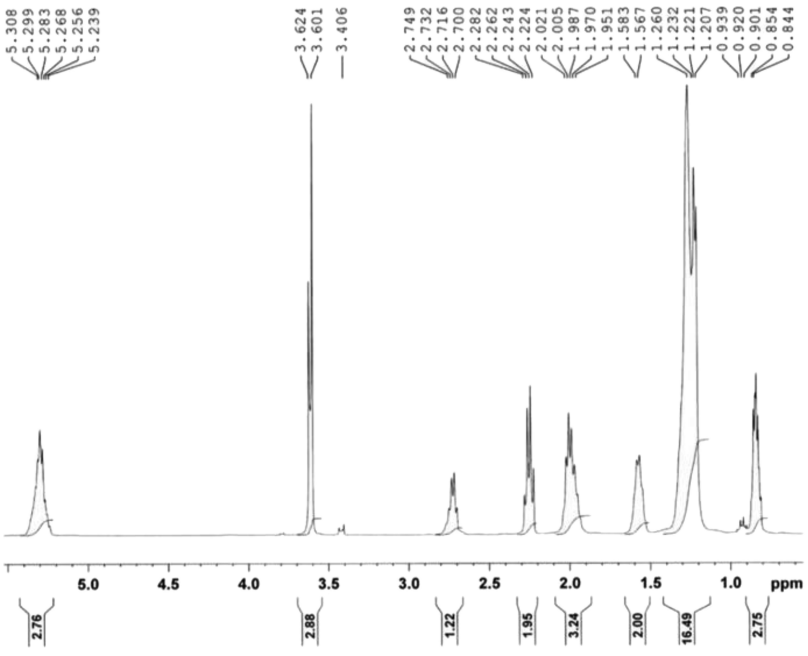


**Figure 7.** $^1$H NMR spectrum of FAME from exp 14.



https://doi.org/10.1021/acsomega.1c05582
ACS Omega 2021, 6, 35679−35691

Table 6. Comparison of Catalytic Performance for the Transesterification Reaction over the CaO, 1.25% $K^+$-CaO, 2.5% $K^+$-CaO, and 5% $K^+$-CaO Catalysts Derived from the 16th Cycle of Waste Frying Soybean Oil

| biodiesel feedstock | source of catalyst | doping (wt %) | catalyst amount (wt %) | reaction temperature (°C) | methanol/oil ratio | reaction time (min) | biodiesel yield (%) | reference |
|---|---|---|---|---|---|---|---|---|
| sunflower oil | egg shell (CaO) | | 5 | 60 | 15:1 | 120 | 73 | 15 |
| Jatropha oil | egg shell (CaO) | | 5 | 65 | 12:1 | 90 | 69.2 | 19 |
| Karanja oil | egg shell (CaO) | | 5 | 65 | 12:1 | 90 | 65.5 | 19 |
| WSO | egg shell (CaO)/KOH | 7 | 1.5 | 65 | 12:1 | 180 | 87.17 | 20 |
| *Madhuca indica* oil | egg shell (CaO)/Na | 5 | 5 | 60 | 9:1 | 120 | 81.1 | 40 |
| Jatropha oil | KOH/CaO | 20 | 3 | 60 | 8:1 | 60 | 97.0 | 11 |
| WCO | egg shell (CaO) | | 5 | 65 | 9:1 | 165 | 87.8 | 41 |
| WCO | egg shell (CaO)/Zn | 1 | 5 | | 20:1 | 240 | 96.74 | 16 |
| WCO | chicken bones (CaO) | | 5 | 65 | 15:1 | 240 | 89.3 | 37 |
| WCO | scallop shell (CaO) | | 5 | 65 | 6:1 | 120 | 86.0 | 38 |
| WSO | egg shell (CaO) | | 3 | 65 | 12:1 | 180 | 88.1 | this study |
| WSO | egg shell (CaO)/KOH | 1.25 | 3 | 65 | 12:1 | 180 | 88.94 | this study |
| WSO | egg shell (CaO)/KOH | 2.50 | 7 | 65 | 12:1 | 240 | 96.96 | this study |
| WSO | egg shell (CaO)/KOH | 5 | 3 | 65 | 12:1 | 180 | 98.46 | this study |

Table 7. Fatty Acid Methyl Ester Conversion in Different Frying Cycles of Soybean Oil[a]

| | soybean oil | | | |
|---|---|---|---|---|
| no. of frying cycle | 4th | 8th | 12th | 16th |
| biodiesel yield | 98.02 | 98.17 | 97.85 | 98.46 |

[a]Reaction conditions: temp, 65 °C; $K^+$ loading, 5% $K^+$-CaO; catalyst amount, 3% (w/w); time, 180 min; and methanol to oil ratio, 12:1.

Table 8. Compositional Analysis of Fatty Acid Methyl Ester Obtained from Different Frying Cycles of Soybean Oil

| FAME | no. of frying cycle | | | |
|---|---|---|---|---|
| | 4th | 8th | 12th | 16th |
| methyl palmitate C16:0 ME | 9.84 | 10.22 | 10.61 | 10.56 |
| methyl stearate C18:0 ME | 4.26 | 4.63 | 5.16 | 5.82 |
| methyl oleate C18:1 ME | 24.98 | 25.13 | 25.54 | 29.54 |
| methyl linoleate C18:2 ME | 51.15 | 50.04 | 49.02 | 46.03 |
| methyl linolenate C18:3 ME | 6.89 | 6.72 | 6.09 | 5.04 |
| methyl arachidate C20:0 ME | 0.25 | 0.07 | 0.26 | 0.28 |
| methyl eicosenoate C20:1 ME | 0.13 | 0.39 | 0.14 | 0.12 |
| methyl behenate C22:0ME | 0.41 | 0.46 | 0.41 | 0.43 |
| methyl lignocerate C24:0 ME | 0.40 | 0.45 | 0.42 | 0.57 |

differences were found among FAME compositions obtained from different frying cycles. However, it is noteworthy that the FAME percentage of polyunsaturated methyl linoleate (C18:2) and methyl linolenate (C18:3) keeps decreasing with the increasing frying cycle, which could be attributed to their degradation at high temperature and increased frying time.[36]

**2.8. Properties of Produced Biodiesel.** The physiochemical properties of the biodiesel obtained from different frying cycles of WSO are outlined in Table 9. The lower kinematic viscosity indicates the suitability of the biodiesel for use in existing engines. On the other hand, the high flash point suggests that the fuel is safe for storage and transportation. The calorific value is also lower than conventional petro-diesel but higher compared to other biodiesels. Additionally, the produced biodiesel's acid value is within the recommended limit, meaning that it is safe for fuel tanks and parts of diesel engines. Therefore, it can be concluded that the produced biodiesel can be used either directly or by blending with petro-diesel.[39]

**2.9. Reusability of the Developed Catalyst.** From the commercial point of view, reuse of the prepared catalyst is a significant criterion for decreasing the operating cost. In this work, the catalyst responsible for the maximum yield was used eight consecutive times to gain insight into the extent to which its activity decreases with each new reuse. After completing the reaction, the reaction mixture was filtered to separate the catalyst and washed with *n*-hexane. The catalyst was dried overnight at 105 °C in an oven and then reactivated by calcination at 900 °C in the muffle furnace for approximately 4 h. Figure 8 shows the

Table 9. Fuel Properties of Prepared Biodiesel Obtained from Different Frying Cycles

| parameter | units | WSO biodiesel | | | | test method | EN 14214:2012 |
|---|---|---|---|---|---|---|---|
| | | 4th | 8th | 12th | 16th | | |
| viscosity @ 40 °C | cSt | 4.52 | 4.58 | 4.55 | 4.59 | ASTM D445-19a | 3.50−5.00 |
| acid value | mgKOH/g | 0.22 | 0.23 | 0.28 | 0.28 | ASTM D664-18e2 | 0.50 max |
| pour point | °C | −11.2 | −14 | −13.4 | −16 | ASTM D97-17b | |
| density @ 25 °C | $Kg/m^3$ | 868.5 | 884.032 | 871.54 | 890.6 | ASTM D4052-18a | 860−900 |
| calorific value (CV) | MJ/kg | 40.45 | 40.49 | 40.02 | 40.12 | ASTM D240-19 | |
| flash point | °C | 161.1 | 162 | 164.1 | 168.1 | ASTM D93-20 | 120 min |



https://doi.org/10.1021/acsomega.1c05582
ACS Omega 2021, 6, 35679−35691

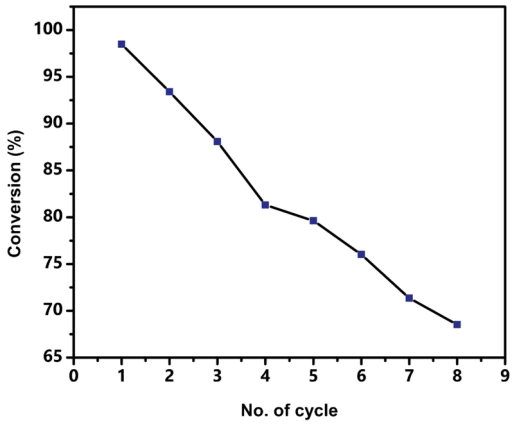


**Figure 8.** Effect of catalyst reuse on the biodiesel yield for the 5% $K^+$-CaO catalyst.

decreasing trend in biodiesel yield with each new reaction, with the yield decreasing from 98.48% for the first reaction to 68.52% for the eighth reaction. This experimental data confers the idea that the as-prepared catalyst can be reactivated and reused successfully for biodiesel yield commercially. The yield decreases steadily from the beginning of the reuse. This decrease in the catalyst's catalytic activity with each new reuse can be attributed to $K^+$ leaching into the reaction mixture or long-chain carbon-containing FAME clotting the catalysts' active sites.

**2.10. XRD Analysis of Reuse Catalyst.** The XRD patterns of the reused catalyst from the fourth and eighth cycles are shown in Figure 9 and compared with that of a freshly prepared

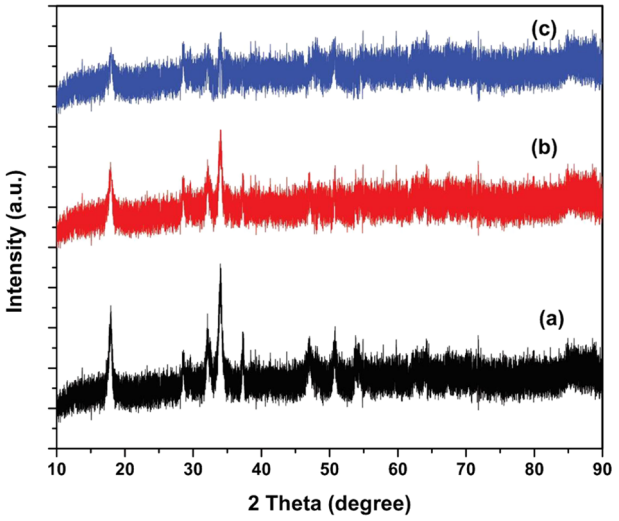


**Figure 9.** XRD patterns of the reused catalyst from the (a) zeroth cycle, (b) fourth cycle, and (c) eighth cycle.

catalyst. It is noticeable that the crystalline nature of the prepared catalysts decreases significantly in the fourth and eighth cycles. Catalyst poisoning can occur by the deposition of reaction products on the catalyst active sites, resulting in the decrease in the crystalline nature of the catalyst.[16]

**2.11. Catalyst Mass Loss during Reuse.** Even though catalyst mass loss is an unavoidable phenomenon during reuse, it is a critical parameter in the commercial point of view. In the current case, the catalyst loss increases in every cycle from the beginning to the last cycle. The eighth cycle has a 58.84%catalyst loss compared to the first cycle shown in Figure 10. However, an average of 7.34% catalyst loss was observed in every cycle of reuse.

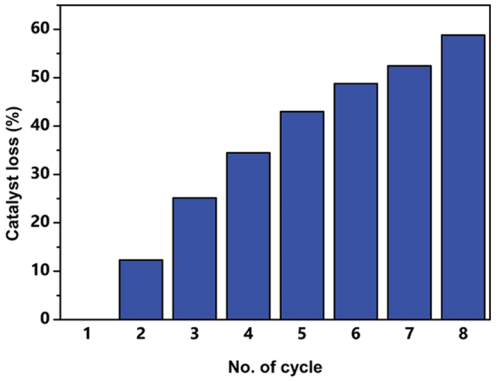


**Figure 10.** Mass loss of the catalyst in every cycle.

## 3. CONCLUSIONS

To fulfill the objective of deriving environmentally benign biodiesel from WSO prepared by frying the oil multiple times, WES-derived CaO and $K^+$-impregnated $K^+$-CaO catalysts were synthesized and characterized by extensive analysis. The catalytic activity of the prepared catalysts was very high, with the 5% $K^+$-CaO catalyst resulting in 98.46% biodiesel conversion under the reaction conditions of 3 wt % catalyst loading, 12:1 methanol to oil molar ratio, and 180 min reaction time at 65 °C reaction temperature. A 5% $K^+$-CaO catalyst was found to be highly reusable, with the biodiesel conversion decreasing by only 30.42% after eight cycles of reuse. Gas chromatography analysis revealed that the difference in FAME composition obtained from different frying cycles was negligible. Various physico-chemical properties of the biodiesel were measured and found to be compatible with the internationally recognized standards. The abundance of WES and the prospect of the WES-derived CaO and $K^+$-CaO catalyst catalyzing the transesterification reaction at relatively low catalyst loading are really phenomenal from an industrial perspective. These catalysts can be used for base catalyzed transesterification of other available feedstocks for efficient and economical production of biodiesel.

## 4. EXPERIMENTAL SECTION

**4.1. Materials.** WES was collected from the BCSIR campus, Dhaka, Bangladesh, and used to synthesize heterogeneous catalyst CaO. A local brand of cooking oil (soybean oil) was purchased from a local market in Dhaka, Bangladesh. Both methanol (99.5%), used for transesterification reaction, and potassium hydroxide, used for metal impregnation, were purchased from Merck, Germany.

**4.2. Preparation of Waste Soybean Oil.** The local brand of soybean oil was turned into WSO by frying potato sticks in it. The temperature of the frying was maintained between 145 and 155 °C. The WSO was collected after every four cycles for a total of 16 frying cycles. Finally, four samples of WSO from the 4th, 8th, 12th, and 16th cycles were collected for investigation.

**4.3. Preparation of the Tested Catalyst.** First, WES were washed with tap water thoroughly to remove the dirt and other organic materials; then, it was rinsed with distilled water and dried in a laboratory air oven at 105 °C or overnight. By pulverizing into smaller particles using a mortar, the dried eggshells' surface area was increased. For making fine particles of


https://doi.org/10.1021/acsomega.1c05582
ACS Omega 2021, 6, 35679−35691

Table 10. Physicochemical Parameter of Fresh and Waste Soybean Oil[a]

| | soybean oil | | | | |
|---|---|---|---|---|---|
| | no. of frying cycle | | | | |
| parameter | fresh | 4th | 8th | 12th | 16th |
| free fatty acid (% g/g) | 0.09 ± 0.01 | 0.22 ± 0.01 | 0.27 ± 0.01 | 0.19 ± 0.02 | 0.28 ± 0.01 |
| viscosity (cst) | 33.53 ± 0.20 | 29.69 ± 0.50 | 29.04 ± 0.50 | 31.82 ± 0.52 | 33.44 ± 0.40 |
| solid content (% g/g) | nil | 0.12 | 0.43 | 0.87 | 1.23 |
| frying time (min) | | 25 | 52 | 77 | 99 |

[a]Conditions: temperature: 150 °C ± 5 °C.

WES, ball milling (FRITSCH pulverisette, Country) was carried out at 200 rpm for 15 min.

Powdered WES were kept in a muffle furnace for calcination at 900 °C for 5 h. Then, the calcinated powdered eggshells were treated with an aqueous solution of potassium hydroxide (1.25, 2.5, and 5% w/w) under constant stirring (600 rpm) at 25 ± 2 °C for 6 h. After impregnation, the solution was kept in the oven at 105 °C for overnight drying. Potassium-impregnated eggshell samples were further calcined in the same muffle furnace for 4 h at a temperature of 900 °C.[10]

The calcined eggshells without metal impregnation were labeled as CaO. The potassium-impregnated calcined eggshells were named 1.25% $K^+$-CaO, 2.5% $K^+$-CaO, and 5% $K^+$-CaO, and for transesterification of WSO, they were used as heterogeneous catalysts.

**4.4. Characterization of Catalyst.** FTIR (Frontier, Perkin-Elmer, UK) analysis, with the KBr pellet method, was carried out in the wavenumber range of 400−4000 $cm^{-1}$ to find out the surface functionalities of the prepared catalysts.

To acquire insights into the crystalline structure, a raw eggshell (RES), CaO, 1.25% $K^+$-CaO, 2.5% $K^+$-CaO, 5% $K^+$-CaO and reused catalyst samples underwent X-ray diffraction (XRD, Bruker D8 Advance, Germany) using Cu K$\alpha$ radiation (I = 0.15405 nm) operated at 40 kV and 40 mA. The XRD patterns were recorded in the 2$\theta$ range of 10 to 90°, with the step size and scan rate being 1.120° and 0.50° $min^{-1}$, respectively.

To determine the surface morphology of the raw eggshell (RES), CaO, 1.25% $K^+$-CaO, 2.5% $K^+$-CaO, and 5% $K^+$-CaO, field emission scanning electron microscopy (FESEM; JSM-7610F, JEOL, Japan) (accelerating voltage: 5 kV, magnification: 15000X) was used to take images. Energy dispersive spectroscopy (EDS; 7610F, JEOL, Japan) (accelerating voltage: 15 kV, magnification: 500×) was used to identify and quantify the elements present in the prepared catalyst samples.

The surface area, pore volume and pore diameter were measured by Brunauer−Emmett−Teller (BET). The BET Sorptometer (201-A, USA) system was used in this experiment with $N_2$ adsorption−desorption at −196 °C. Before analyzing, the samples were heated at 120 °C overnight to degas the pores.

Particle size distribution was measured by a Mastersizer 3000 with a laser diffraction analyzer (Malvern Panalytical Ltd., Malvern, UK). The particles of CaO and 5% $K^+$-CaO catalysts were suspended in deionized water after setting the refractive index at 1.830, and the laser obscuration rate was fixed at 4.01% for analysis.

**4.5. Biodiesel Preparation Using the Prepared Catalysts.** First, the WSO was filtered to remove the solid impurities. The FFA content was measured by titrating all the test WSO samples against 0.1 N aqueous potassium hydroxide solution according to the standard procedure. Since all the tested samples had FFA values lower than 2% as shown in Table 10, the 16th cycle WSO was selected based on FFA and solid contents for the transesterification process.[3] Selected WSO samples were subjected to the transesterification reaction in the presence of three different catalysts (1.25% $K^+$-CaO, 2.5% $K^+$-CaO, and 5% $K^+$-CaO) and methanol under other process conditions as presented in Table 5. Transesterifications were carried out in a bioreactor arranged with a three-neck flat bottom round flask. The flask was fitted with a thermometer and a water condensation facility. First, the oil feedstock (20 g) was added to the flask and it was then placed onto a heating mantle. The reaction temperature was maintained at 65 ± 2 °C, with a magnetic stirrer rotating inside the flask at 600 rpm. Methanol and catalysts were added in different experimental amounts after the temperature of the oil reached 65 °C. After the reaction was completed, the product mixture was taken out of the reactor and the catalyst was separated from the mixture by filtration. Later, excess methanol was evaporated and the treated oil was taken into a separating funnel. The glycerol layer was in the bottom part, and finally, the fatty acid methyl ester (FAME)-rich layer was on the top of the separating funnel.

**4.6. Gas Chromatography (GC) Analysis.** Agilent 6890 N Gas Chromatography (USA), equipped with a flame ionization detector (FID), was used for the determination of the FAME composition of the prepared biodiesel sample according to EN 14103. The sample was passed through a DB-5HT column (30 m × 0.25 mm × 0.25 $\mu$m) for compositional analysis.

**4.7. $^1$H NMR Analysis.** FAME conversion was inspected by $^1$H NMR using a 400 MHz FT-NMR spectrometer (Bruker 400 ASCEND, Germany). The conversion rate of prepared FAME was determined using eq 3,[42] where $C$ is the percentage conversion of triglycerides to corresponding methyl esters. $A_{ME}$ represents the integration value of methoxy protons of the methyl ester moiety and $A_{\alpha-CH_2}$ highlights the integration value of the $\alpha$-methylene protons.

$$C(\%) = \frac{2A_{ME}}{3A_{\alpha-CH_2}} \times 100 \quad (3)$$

**4.8. Design of the Experiment.** *4.8.1. Experimental Design and Statistical Analysis.* To minimize the number of experiments to save resources and time and to study the interaction between process variables leading to maximum biodiesel conversion, BBD-based RSM was evaluated using Minitab statistical software (Minitab, LLC, Pennsylvania, USA). Four reaction parameters, namely, doping of $K^+$ (A), amount of catalyst (B), methanol to oil ratio (C), and reaction time (D), were varied, and their impacts on the maximum biodiesel conversion were evaluated utilizing regression and graphical analysis. The coded levels of the reaction parameters along with the experimental ranges are mentioned in Table 11, where −1, 0, and 1 signify the low level, center point, and high level, respectively, of the coded values. A total of 28 experiments were


https://doi.org/10.1021/acsomega.1c05582
ACS Omega 2021, 6, 35679−35691

**Table 11. Selected Variables and Coded Levels Used in the BBD**

| variables | symbol | coded levels | | |
|---|---|---|---|---|
| | | −1 | 0 | +1 |
| $K^+$-doping (%) | A | 1.25 | 2.5 | 5 |
| catalyst amount (%) | B | 3 | 5 | 7 |
| methanol:oil (mol) | C | 9:1 | 12:1 | 15:1 |
| reaction time (min) | D | 120 | 180 | 240 |

carried out, keeping the temperature and stirring speed fixed at 65 °C and 600 rpm, respectively. The predicted response, i.e., FAME yield or biodiesel conversion ($Y$), which is a function of independent variables and their interactions, was analyzed by means of using the following second-order polynomial equation eq 4:

$$Y_{\text{biodiesel conversion}(\%)} = \beta_\circ + \sum_{j=1}^{k} \beta_j X_j + \sum_{j=1}^{k} \beta_{jj} X_j^2 + \sum_{i=1}^{j-1} \sum_{j=2}^{k} \beta_{ij} X_i X_j + \varepsilon \quad (4)$$

In eq 4, $Y$ represents the predicted biodiesel conversion, $k$ is the number of factors studied and optimized in the experiment, $i$ and $j$ are the linear and quadratic coefficients, respectively, $X_i$ and $X_j$ are the uncoded independent variables, $\beta_\circ$ is the regression coefficient, and $\varepsilon$ is the experimental error. Analysis of variance (ANOVA), with a significance level of 5%, was used to validate the model and study the effect and interaction of process variables on the FAME yield.

## ■ ASSOCIATED CONTENT

### Supporting Information

The Supporting Information is available free of charge at https://pubs.acs.org/doi/10.1021/acsomega.1c05582.

XRD pattern of RES, FESEM image of RES, EDS spectra with the corresponding FESEM image of RES, and $^1$H NMR spectrum of FAME from different experiments (PDF)

## ■ AUTHOR INFORMATION


### Corresponding Author

**Mosharof Hossain** − *Department of Environmental Sciences, Jahangirnagar University, Dhaka 1342, Bangladesh; Institute of Fuel Research and Development, Bangladesh Council of Scientific and Industrial Research (BCSIR), Dhaka 1205, Bangladesh;* orcid.org/0000-0003-0834-4740; Phone: +8801741511376; Email: mosharof@bcsir.gov.bd

### Authors

**Nuzhat Muntaha** − *Institute of Fuel Research and Development, Bangladesh Council of Scientific and Industrial Research (BCSIR), Dhaka 1205, Bangladesh*

**Lipiar Khan Mohammad Osman Goni** − *Institute of Fuel Research and Development, Bangladesh Council of Scientific and Industrial Research (BCSIR), Dhaka 1205, Bangladesh*

**Mohammad Shah Jamal** − *Institute of Fuel Research and Development, Bangladesh Council of Scientific and Industrial Research (BCSIR), Dhaka 1205, Bangladesh*

**Mohammad Abdul Gafur** − *Pilot Plant and Process Development Center, Bangladesh Council of Scientific and Industrial Research (BCSIR), Dhaka 1205, Bangladesh*

**Dipa Islam** − *Biomedical and Toxicological Research Institute, Bangladesh Council of Scientific and Industrial Research (BCSIR), Dhaka 1205, Bangladesh*

**Abu Naieum Muhammad Fakhruddin** − *Department of Environmental Sciences, Jahangirnagar University, Dhaka 1342, Bangladesh*

Complete contact information is available at: https://pubs.acs.org/10.1021/acsomega.1c05582


### Author Contributions

The manuscript was written through contributions of all authors. All authors have given approval to the final version of the manuscript.

### Notes

The authors declare no competing financial interest.

## ■ ACKNOWLEDGMENTS

The authors are grateful to Institute of Fuel Research and Development (IFRD), Bangladesh Council of Scientific and Industrial Research (BCSIR), Dhaka-1205, Bangladesh, for laboratory support. The authors also appreciate the technical support from Md. Saiful Quddus, Scientific Officer, and Md. Farid Ahmed, Scientific Officer, Institute of Glass and Ceramic Research and Testing, BCSIR, Dhaka-1205, Bangladesh. The authors are thankful to Bangabandhu Science and Technology Fellowship Trust under the Ministry of Science and Technology, the Peoples Republic of Bangladesh, for providing fellowship.

## ■ ABBREVIATIONS

| | |
|---|---|
| FAME | fatty acid methyl ester |
| FFA | free fatty acid |
| WCO | waste cooking oil |
| RES | raw eggshell |
| WES | waste eggshell |
| WSO | waste soybean oil |

## ■ REFERENCES


(1) Yadav, M.; Singh, V.; Sharma, Y. C. Methyl Transesterification of Waste Cooking Oil Using a Laboratory Synthesized Reusable Heterogeneous Base Catalyst: Process Optimization and Homogeneity Study of Catalyst. *Energy Convers. Manage.* **2017**, *148*, 438−1452.

(2) Alam, M.; Rana, S.; Haque, M.; Hossain, M.; Sujan, S.; Jamal, M. Biodiesel from Non-Edible Karanja Seed Oil. *Bangladesh J. Sci. Ind. Res.* **2017**, *52*, 15−20.

(3) Hossain, M.; Moniruzzaman, M.; Sujan, S. M. A.; Hossain, M.; Jamal, M. S. Extraction of Crude Rubber Oil from Rubber Seed and Production of Biodiesel. *Biofuels* **2014**, *5*, 16−23.

(4) Dhawane, S. H.; Kumar, T.; Halder, G. Parametric Effects and Optimization on Synthesis of Iron (II) Doped Carbonaceous Catalyst for the Production of Biodiesel. *Energy Convers. Manage.* **2016**, *122*, 310−320.

(5) Rana, S.; Haque, M.; Poddar, S.; Sujan, S.; Hossain, M.; Jamal, M. Biodiesel Production from Non-Edible Mahogany Seed Oil by Dual Step Process and Study of Its Oxidation Stability. *Bangladesh J. Sci. Ind. Res.* **2015**, *50*, 77−86.

(6) Bora, A. P.; Dhawane, S. H.; Anupam, K.; Halder, G. Biodiesel Synthesis from Mesua Ferrea Oil Using Waste Shell Derived Carbon Catalyst. *Renewable Energy* **2018**, *121*, 195−204.

(7) Dhawane, S. H.; Chowdhury, S.; Halder, G. Lipase Immobilised Carbonaceous Catalyst Assisted Enzymatic Transesterification of

*Mesua Ferrea* Oil. *Energy Convers. Manage.* **December 2018**, *2019*, 671−680.
(8) Dhawane, S. H.; Kumar, T.; Halder, G. Central Composite Design Approach towards Optimization of Flamboyant Pods Derived Steam Activated Carbon for Its Use as Heterogeneous Catalyst in Transesterification of Hevea Brasiliensis Oil. *Energy Convers. Manage.* **2015**, *100*, 277−287.
(9) Fonseca, J. M.; Teleken, J. G.; de Cinque Almeida, V.; da Silva, C. Biodiesel from Waste Frying Oils: Methods of Production and Purification. *Energy Convers. Manage.* **2019**, *184*, 205−218.
(10) Joshi, G.; Rawat, D. S.; Lamba, B. Y.; Bisht, K. K.; Kumar, P.; Kumar, N.; Kumar, S. Transesterification of Jatropha and Karanja Oils by Using Waste Egg Shell Derived Calcium Based Mixed Metal Oxides. *Energy Convers. Manage.* **2015**, *96*, 258−267.
(11) Liao, C.-C.; Chung, T.-W. Optimization of Process Conditions Using Response Surface Methodology for the Microwave-Assisted Transesterification of Jatropha Oil with KOH Impregnated CaO as Catalyst. *Chem. Eng. Res. Des.* **2013**, *91*, 2457−2464.
(12) Bedir, Ö.; Doğan, T. H. Use of Sugar Industry Waste Catalyst for Biodiesel Production. *Fuel* **2021**, *286*, 119476.
(13) Ramachandran, K.; Sivakumar, P.; Suganya, T.; Renganathan, S. Production of Biodiesel from Mixed Waste Vegetable Oil Using an Aluminium Hydrogen Sulphate as a Heterogeneous Acid Catalyst. *Bioresour. Technol.* **2011**, *102*, 7289−7293.
(14) Yusuff, A. S. Characterization of Alkaline Modified Anthill and Investigation of Its Catalytic Behaviour in Transesterification of *Chrysophyllum Albidium* Seed Oil. *S. Afr. J. Chem. Eng.* **2019**, *29*, 24−32.
(15) Bedir, Ö.; Doğan, T. H. Comparison of Catalytic Activities of Ca-Based Catalysts from Waste in Biodiesel Production. *Energy Sources, Part A* **2021**, *00*, 1−18.
(16) Borah, M. J.; Das, A.; Das, V.; Bhuyan, N.; Deka, D. Transesterification of Waste Cooking Oil for Biodiesel Production Catalyzed by Zn Substituted Waste Egg Shell Derived CaO Nanocatalyst. *Fuel* **2019**, *242*, 345−354.
(17) Dhawane, S. H.; Kumar, T.; Halder, G. Insight into Biodiesel Synthesis Using Biocatalyst Designed through Lipase Immobilization onto Waste Derived Microporous Carbonaceous Support. *Process Saf. Environ. Prot.* **2019**, *124*, 231−239.
(18) Rahman, W. U.; Fatima, A.; Anwer, A. H.; Athar, M.; Khan, M. Z.; Khan, N. A.; Halder, G. Biodiesel Synthesis from Eucalyptus Oil by Utilizing Waste Egg Shell Derived Calcium Based Metal Oxide Catalyst. *Process Saf. Environ. Prot.* **2019**, *122*, 313−319.
(19) Degfie, T. A.; Mamo, T. T.; Mekonnen, Y. S. Optimized Biodiesel Production from Waste Cooking Oil (WCO) Using Calcium Oxide (CaO) Nano-Catalyst. *Sci. Rep.* **2019**, *9*, 1−8.
(20) Oko, S.; Syahrir, I.; Irwan, M. The Utilization of CaO Catalyst Impregnated with KOH in Biodiesel Production from Waste Cooking Oil. *Int. J. Sci. Technol. Res.* **2018**, *7*, 115−118.
(21) Kusmiyati, K.; Prasetyoko, D.; Murwani, S.; Fadhilah, M. N.; Oetami, T. P.; Hadiyanto, H.; Widayat, W.; Budiman, A.; Roesyadi, A. Biodiesel Production from *Reutealis Trisperma* Oil Using KOH Impregnated Eggshell as a Heterogeneous Catalyst. *Energies.* **2019**, *12*, 3714.
(22) Hsiao, M. C.; Lin, C. C.; Chang, Y. H. Microwave Irradiation-Assisted Transesterification of Soybean Oil to Biodiesel Catalyzed by Nanopowder Calcium Oxide. *Fuel* **2011**, *90*, 1963−1967.
(23) Vujicic, D.; Comic, D.; Zarubica, A.; Micic, R.; Boskovic, G. Kinetics of Biodiesel Synthesis from Sunflower Oil over CaO Heterogeneous Catalyst. *Fuel* **2010**, *89*, 2054−2061.
(24) Mirghiasi, Z.; Bakhtiari, F.; Darezereshki, E.; Esmaeilzadeh, E. Preparation and Characterization of CaO Nanoparticles from Ca-$(OH)_2$ by Direct Thermal Decomposition Method. *J. Ind. Eng. Chem.* **2014**, *20*, 113−117.
(25) Roy, A.; Bhattacharya, J. Microwave assisted synthesis of CaO nanoparticles and use in waste water treatment. *NanoTechnol.* **2011**, *3*, 565−568.
(26) Choudhury, B.; Dey, M.; Choudhury, A. Defect Generation, *d-d* Transition, and Band Gap Reduction in Cu-Doped $TiO_2$ Nanoparticles. *Int. Nano Lett.* **2013**, *3*, 2−9.
(27) Dhawane, S. H.; Bora, A. P.; Kumar, T.; Halder, G. Parametric Optimization of Biodiesel Synthesis from Rubber Seed Oil Using Iron Doped Carbon Catalyst by Taguchi Approach. *Renewable Energy* **2017**, *105*, 616−624.
(28) Niju, S.; Rabia, R.; Sumithra Devi, K.; Naveen Kumar, M.; Balajii, M. Modified Malleus Malleus Shells for Biodiesel Production from Waste Cooking Oil: An Optimization Study Using Box−Behnken Design. *Waste Biomass Valoriz.* **2020**, *11*, 793−806.
(29) Tan, Y. H.; Abdullah, M. O.; Nolasco-Hipolito, C.; Taufiq-Yap, Y. H. Waste Ostrich- and Chicken-Eggshells as Heterogeneous Base Catalyst for Biodiesel Production from Used Cooking Oil: Catalyst Characterization and Biodiesel Yield Performance. *Appl. Energy.* **2015**, *160*, 58−70.
(30) Tshizanga, N.; Aransiola, E. F.; Oyekola, O. Optimisation of Biodiesel Production from Waste Vegetable Oil and Eggshell Ash. *S. Afr. J. Chem. Eng.* **2017**, *23*, 145−156.
(31) Issariyakul, T.; Dalai, A. K. Biodiesel from Vegetable Oils. *Renewable Sustainable Energy Rev.* **2014**, *31*, 446−471.
(32) Kamel, D. A.; Farag, H. A.; Amin, N. K.; Fouad, Y. O. Biodiesel Synthesis from Non-Edible Oils by Transesterification Using the Activated Carbon as Heterogeneous Catalyst. *Int. J. Environ. Sci. Technol.* **2017**, *14*, 785−794.
(33) Monteiro, M. R.; Ambrozin, A. R. P.; Lião, L. M.; Ferreira, A. G. Determination of Biodiesel Blend Levels in Different Diesel Samples by $^1$H NMR. *Fuel* **2009**, *88*, 691−696.
(34) Nongbe, M. C.; Ekou, T.; Ekou, L.; Yao, K. B.; Le Grognec, E.; Felpin, F. X. Biodiesel Production from Palm Oil Using Sulfonated Graphene Catalyst. *Renewable Energy* **2017**, *106*, 135−141.
(35) Tariq, M.; Ali, S.; Ahmad, F.; Ahmad, M.; Zafar, M.; Khalid, N.; Khan, M. A. Identification, FT-IR, NMR ($^1$H and $^{13}$C) and GC/MS Studies of Fatty Acid Methyl Esters in Biodiesel from Rocket Seed Oil. *Fuel Process. Technol.* **2011**, *92*, 336−341.
(36) Kinney, A. J.; Clemente, T. E. Modifying Soybean Oil for Enhanced Performance in Biodiesel Blends. *Fuel Process. Technol.* **2005**, *86*, 1137−1147.
(37) Knothe, G. A Comprehensive Evaluation of the Cetane Numbers of Fatty Acid Methyl Esters. *Fuel* **2014**, *119*, 6−13.
(38) Chowdhury, S.; Dhawane, S. H.; Jha, B.; Pal, S.; Sagar, R.; Hossain, A.; Halder, G. Biodiesel Synthesis from Transesterified Madhuca Indica Oil by Waste Egg Shell−Derived Heterogeneous Catalyst: Parametric Optimization by Taguchi Approach. *Biomass Convers. Biorefin.* **2021**, *11*, 1171−1181.
(39) Peng, Y.-P.; Amesho, K. T. T.; Chen, C.-E.; Jhang, S.-R.; Chou, F.-C.; Lin, Y.-C. Optimization of Biodiesel Production from Waste Cooking Oil Using Waste Eggshell as a Base Catalyst under a Microwave Heating System. *Catalysts* **2018**, *8*, 1−16.
(40) Farooq, M.; Ramli, A.; Naeem, A. Biodiesel Production from Low FFA Waste Cooking Oil Using Heterogeneous Catalyst Derived from Chicken Bones. *Renewable Energy* **2015**, *76*, 362−368.
(41) Sirisomboonchai, S.; Abuduwayiti, M.; Guan, G.; Samart, C.; Abliz, S.; Hao, X.; Kusakabe, K.; Abudula, A. Biodiesel Production from Waste Cooking Oil Using Calcined Scallop Shell as Catalyst. *Energy Convers. Manage.* **2015**, *95*, 242−247.
(42) Boro, J.; Konwar, L. J.; Thakur, A. J.; Deka, D. Ba Doped CaO Derived from Waste Shells of T Striatula (TS-CaO) as Heterogeneous Catalyst for Biodiesel Production. *Fuel* **2014**, *129*, 182−187.


https://doi.org/10.1021/acsomega.1c05582
*ACS Omega* 2021, 6, 35679−35691